Organic Process Research & Development

Article

pubs.acs.org/OPRD

Modeling-Based Approach Towards Quality by Design for the Ibipinabant API Step

Shawn B. Brueggemeier,* Emily A. Reiff, Olav K. Lyngberg, Lindsay A. Hobson, and Jose E. Tabora

Chemical Development, Bristol-Myers Squibb Company, One Squibb Drive, New Brunswick, New Jersey 08903, United States

ABSTRACT: This work presents a process modeling-based methodology towards quality by design that was applied throughout the development lifecycle of the ibipinabant API step. By combining mechanistic kinetic modeling with fundamental thermodynamics, the degradation of the API enantiomeric purity was described across a large multivariate process knowledge space. This knowledge space was then narrowed down to the process design space through risk assessment, target quality specifications, practical operating conditions for scale-up, and plant control capabilities. Subsequent analysis of process throughput and yield defined the target operating conditions and normal operating ranges for a specific pilot-plant implementation. Model predictions were verified via results obtained in the laboratory and at pilot-plant scale. Future efforts were focused on increasing fundamental process knowledge, improving model confidence, and using a risk-based approach to reevaluate the design space and selected operating conditions for the next scale-up campaign.

INTRODUCTION

The quality by design (QbD) initiative aims to ensure pharmaceutical product quality via scientific and process understanding, risk management, critical quality attribute (CQA) control strategies, and multivariate design space definition.[1−4] In contrast to the traditional approach of demonstrated process reproducibility and testing of the final product, "quality should be built in by design" within the QbD paradigm.[5−7] While QbD is a potential aspect of the regulatory filing, the foundations of a QbD filing are created throughout the process development lifecycle (Figure 1). Process data

Figure 1. Pharmaceutical quality by design (QbD) methodology.

generated early in development aid in process evaluation and enable prioritization of development activities. As development continues, the breadth of scientific process understanding increases as do the requirements on the accuracy and extent of design space understanding.[8] In order to turn process data into process knowledge, data visualization and process modeling are employed to enable predictive capabilities. New process knowledge is then used to modify the existing process or control strategy and update the resulting design space. It is recognized that full and comprehensive design space understanding is neither feasible nor practical, especially at earlier stages of development, and risk-based evaluations focus the development efforts to the highest risk process aspects.[9]

In this contribution we describe a process modeling-based approach to QbD for the ibipinabant active pharmaceutical ingredient (API) step. Ibipinabant was in development as a cannabinoid CB-1 receptor antagonist for the treatment of obesity.[10,11] Within the chemical development group, the compound transitioned from a 6-kg delivery of API for toxicology studies and drug product formulation development to a 175-kg delivery of API for late-stage clinical trials. Throughout the program's life cycle, the focus of the process development team was to generate sufficient process understanding to enable risk assessments, define the design space that was "fit-for-purpose" given the corresponding stage of development, address scale-up control limitations by adjusting the target operating ranges, and implement effective control strategies. In the case study presented here, this methodology was applied in particular to understand and control undesired degradation of enantiomeric purity during the API crystallization. What follows is a description of the implemented work flow along with the kinetic and thermodynamic process models developed to support the underlying QbD approach.

Description of the API Step and the Starting Point for This Case Study. The starting point for this case study was the API process utilized in the first pilot-plant campaign (Scheme 1). In this process, the aspartic acid salt of the final intermediate (**1**) was initially converted to the free base in sodium hydroxide and methylene chloride. Following a phase separation, the rich organic stream was washed with water and then reacted with 4-chlorobenzenesulfonyl chloride (SuCl) using biphasic Schotten−Baumann conditions. The excess 4-chlorobenzenesulfonyl

Received: October 21, 2011
Published: March 13, 2012

   dx.doi.org/10.1021/op2003024 | *Org. Process Res. Dev.* 2012, 16, 567−576

Scheme 1. API process at the time of the first pilot-plant campaign

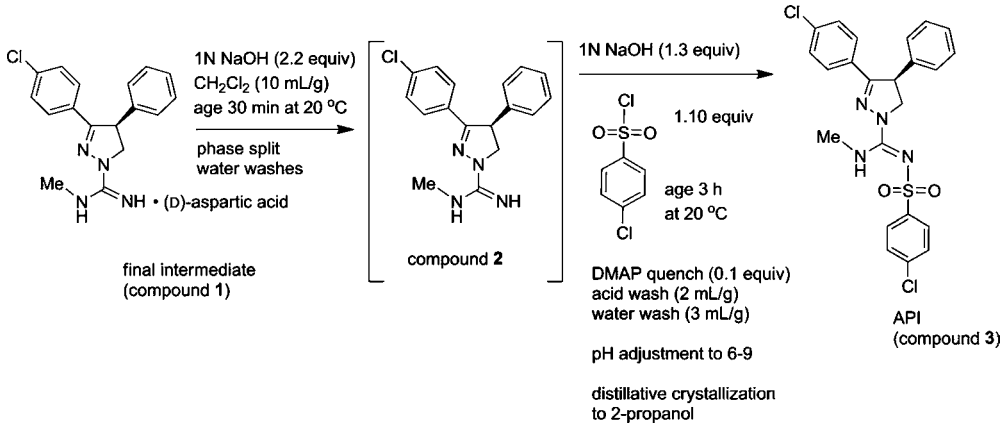

Scheme 2. Process for the second pilot-plant implementation[a]

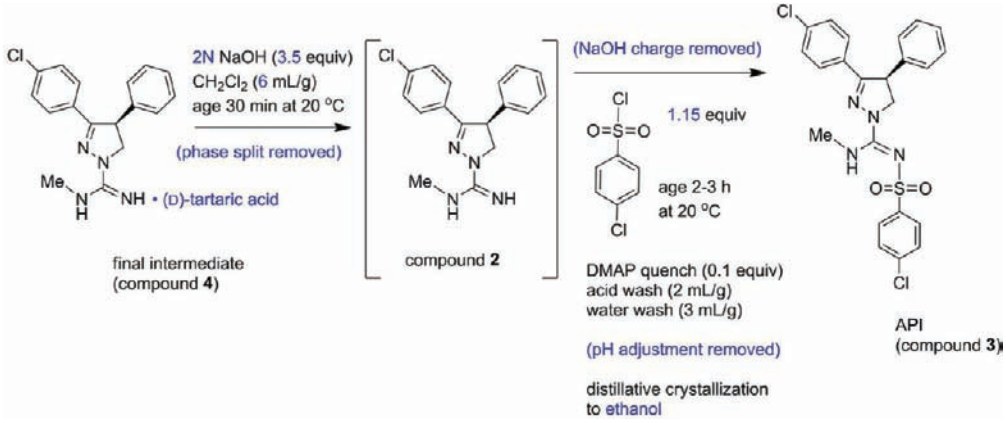

[a]Changes from the previous process are highlighted in blue.

chloride was removed using 4-dimethylaminopyridine (DMAP), the rich organic layer was washed with acid and water, and the rich organic layer was adjusted to neutral pH. The rich organic stream was then subjected to a distillative crystallization by a solvent exchange to 2-propanol in order to provide the crystalline API (**3**).

In preparation for the next pilot-plant campaign, several changes were made to the API process (Scheme 2). The final intermediate was changed from an aspartic acid salt to a tartaric acid salt. The phase separation and washes between the formation of the free base and sulfonylation reaction were removed, and these steps were run more concentrated. The pH adjustment prior to the solvent exchange was removed. Finally, the antisolvent for the distillative crystallization was changed from 2-propanol to ethanol. While the rationale behind each individual change will not be discussed in detail here, the modifications collectively provided an increase in process robustness and throughput, and a simplification of the analytical burden during API release testing.

At this point in development, sufficient process knowledge existed to identify potential critical quality attributes (CQAs) of the API and to begin prioritizing these CQAs by risk. The proposed CQAs for the drug substance were identified as chiral purity, genotoxic impurity profile, chemical purity profile, residual solvents, potency, color, form, and particle size; the performance of the modified API process against these CQAs was assessed via a quality risk assessment using failure mode and effect analysis (FMEA). Twelve high-priority failure modes were identified which can be broadly categorized into genotoxic impurity control strategy and insufficient understanding of the process design space. In order to address the risks associated with insufficient process design space understanding, approximately 20 individual lab experiments were conducted on the new process (Scheme 2). These were single-goal experiments conducted at 10−400 g scale for general process development purposes and were not part of a systematic study incorporating design of experiments (DOE). The experimental conditions along with the typical results are shown in Figure 2. Although the sulfonylation reaction was typically complete (<1 HPLC area percent (AP) of **2** remaining) within 3 h and provided product with >99.85 AP purity and >99.9% ee, a few experiments conducted near the limits of the parameter ranges had unexpected results. Four experiments showed lower than expected reaction conversion (2−4 AP of **2** remaining), and one experiment resulted in API with unacceptable enantiomeric purity (30% ee). Initial analysis of this data set suggested that high levels of **2** at the end of the sulfonylation reaction could lead to racemization of the API in the subsequent distillative crystallization. At this point, one response could have been to narrow the parameter range to the subset of experimental conditions providing acceptable API quality and proceed forward. Instead, we sought to understand the observed process performance via the development of process models for the sulfonylation reaction and the distillative crystallization. We

dx.doi.org/10.1021/op2003024 | *Org. Process Res. Dev.* 2012, 16, 567−576

3.0 – 4.0 equiv NaOH
5 – 12 mL/g CH_2Cl_2
5 – 35 °C
1.0 – 1.2 equiv 4-chlorobenzenesulfonyl chloride
atmospheric distillation
1.8 – 8 h distillation length

⇩ typical results

< 1 AP residual compound **2** at 3 h
> 99.85 AP
> 99.9 %ee
84 – 88 % yield

Figure 2. Process parameter ranges and typical results from approximately 20 lab experiments conducted on the process shown in Scheme 2.

combined these models with an understanding of the chiral purity which was identified as the highest risk CQA through a process risk assessment and analysis of the existing experimental data. The goal was to then utilize the process models and CQA understanding to guide further design space definition as well as the development of the desired process operating ranges for the next pilot-plant campaign. A general strategy in building the design space is to address the most restrictive CQA while, in parallel, verifying acceptable performance of the remaining CQAs. As chiral purity was determined to be the most restrictive CQA, its control and understanding is discussed in depth here, and development efforts focused on understanding and controlling the remaining CQAs are not discussed.

Development of a Kinetic Model for the Sulfonylation Reaction. The initial step in the creation of a process model for the sulfonylation reaction was generation of an Ishikawa diagram (Figure 3). Potential factors affecting the level of **2** include reaction concentration, reaction temperature, equivalents of 4-chlorobenzenesulfonyl chloride, potency of the input material (wt/wt %), equivalents of NaOH, reaction time, mixing within the biphasic system, source of the input materials, and additional quality attributes of the input reagents and/or solvents.[12] On the basis of the existing process knowledge, the first six of these nine factors were selected for model building and were translated into the simple kinetic model shown below. Only if a model built from these factors failed to adequately describe the sulfonylation reaction performance across the existing data set would additional factors be incorporated into the model.

Mechanistically, the reaction produces HCl as a side product which must be sequestered for the reaction to continue. Therefore, the model takes into account the amount of NaOH relative to the extent of reaction conversion as follows:

Reaction rate when the total moles of NaOH are greater than the moles of HCl produced via reaction:

$$r_1 = \text{rate of formation of API}$$
$$= k[2] \times [\text{4-chlorobenzenesulfonyl chloride}]$$

where $k = k_1 \times \exp(-E_{a,1}/RT)$, $k_1 = 1.49 \times 10^{-2}$ L/mol/s ± 8.5%, $E_{a,1} = 47.96$ kJ/mol ± 21%, $T_{ref} = 25$ °C

Otherwise:

For simplicity, we assumed the reaction rate to be zero when the total moles of NaOH are less than the moles of HCl produced via reaction:

$$r_1 = 0$$

Using DynoChem software from Scale-up Systems Ltd., the API reaction kinetic model was fit to the previously existing experimental data. The data was divided into a model-building calibration set ($N = 9$), which was used to regress the model parameters shown above, and a validation set ($N = 5$), which was used to verify the accuracy of the model. The calibration data set and resulting model fit are shown in Figure 4. A parity plot of reaction conversion results for the model building, model verification, and pilot-plant scale-up data sets is shown in Figure 5, and error statistics for the model are provided in Table 1.

Development of a Hybrid Thermodynamic/Kinetic Model for the Degradation of Enantiomeric Purity during the Distillative Crystallization. The Ishikawa

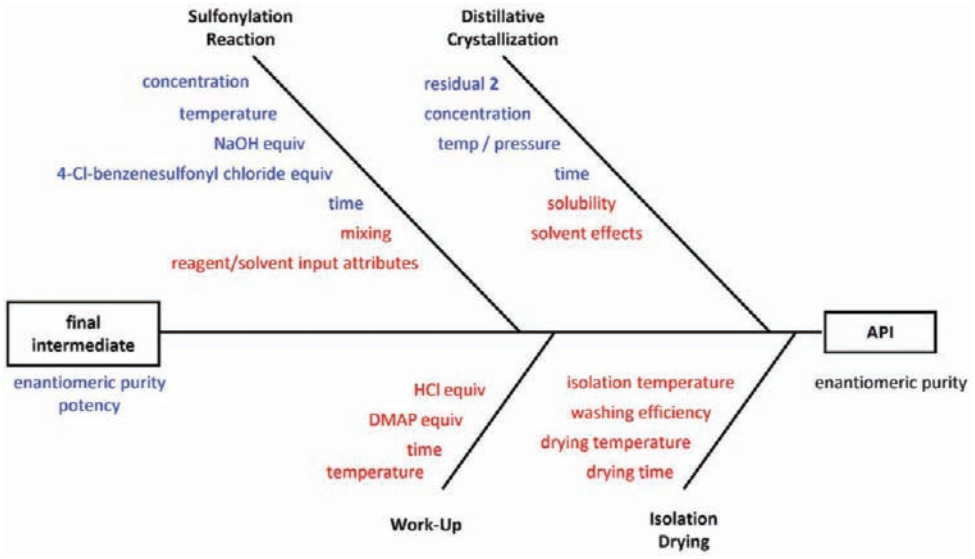

Figure 3. Ishikawa diagram for the API step, highlighting factors that potentially affect the enantiomeric purity of the product. Factors shown in blue were accounted for in the sulfonylation reaction and distillative crystallization models. Factors shown in red were not included in the models.

dx.doi.org/10.1021/op2003024 | Org. Process Res. Dev. 2012, 16, 567–576

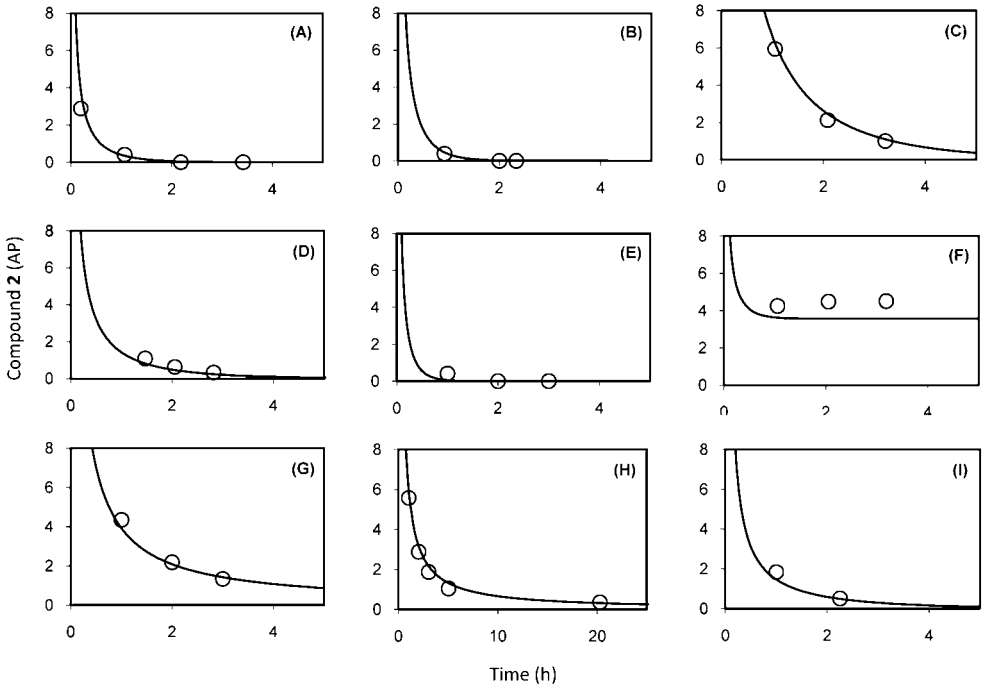

Figure 4. Sulfonylation reaction conversion profiles for the nine model-building experiments. Solid lines represent the model prediction, and open circles represent the experimental values. Experimental conditions are: (A) 35 °C, 1.13 equiv 4-chlorobenzenesulfonyl chloride, 6 mL/g; (B) 20 °C, 1.09 equiv 4-chlorobenzenesulfonyl chloride, 5.5 mL/g; (C) 5 °C, 1.12 equiv 4-chlorobenzenesulfonyl chloride, 10 mL/g; (D) 20 °C, 1.10 equiv 4-chlorobenzenesulfonyl chloride, 5 mL/g; (E) 30 °C, 1.12 equiv 4-chlorobenzenesulfonyl chloride, 6 mL/g; (F) 35 °C, 0.94 equiv 4-chlorobenzenesulfonyl chloride, 5 mL/g; (G) 10 °C, 1.09 equiv 4-chlorobenzenesulfonyl chloride, 4.5 mL/g; (H) 10 °C, 1.00 equiv 4-chlorobenzenesulfonyl chloride, 8 mL/g; (I) 20 °C, 1.03 equiv 4-chlorobenzenesulfonyl chloride, 6 mL/g.

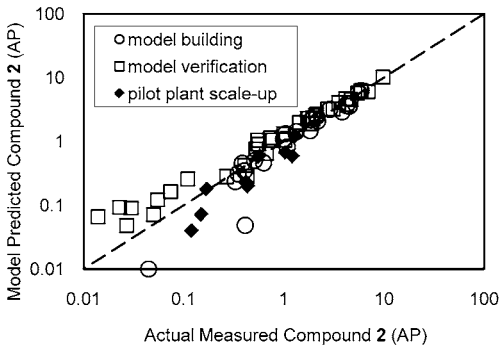

Figure 5. Parity plot for sulfonylation reaction conversion.

diagram for the degradation of API enantiomeric purity is shown in Figure 3. Scientific intuition, current process knowledge, and the risk assessment identified the distillative crystallization as the highest risk unit operation for ee degradation. Potential factors affecting the rate of degradation during the distillative crystallization include residual **2**, concentration, distillation temperature (which is determined by the distillation pressure and solvent composition), distillation time, API solubility, and modulation of the racemization reaction rate due to changing solvent composition during the distillation.[13] Modeling of the system is complicated by the fact that the batch temperature, concentration, and solvent ratio are changing during the distillation. Additionally, the mechanism of racemization was not fully understood at the time of model development although a base-mediated deprotonation of the API chiral center was suspected. Given these factors, a hybrid thermodynamic/kinetic model was pursued rather than a fundamental kinetic model as was generated for the sulfonylation reaction.

Table 1. Sulfonylation reaction model error for the model building and model verification data sets

	model bldg (entire data set)	model ver. (entire data set)	model bldg (ROI[a])	model ver. (ROI[a])
rms[b] error (AP)	0.40	0.42	0.19	0.36
mean rel. error (%)	16.3	24.4	24.4	28.1
mean abs. error (AP)	0.29	0.25	0.14	0.20
max. abs. error (AP)	0.95	0.97	0.36	0.57

[a]For error analysis, the ROI (region of interest) includes points in which the level of **2** was ≤2.0 AP. [b]rms = root mean square.

In order to capture the changing batch temperature profile throughout the course of the distillation exchanging methylene chloride for ethanol, as well as the dependence of this temperature profile on the distillation pressure, a simple batch distillation model was constructed in DynoChem. The model described vapor−liquid−equilibrium via Antoine coefficients and UNIFAC activity coefficients for the two solvents. Mass and energy balances were incorporated to account for changes in the product concentration and solvent ratio as well as to capture the cycle time of the distillation based on specific vessel heat transfer coefficients and jacket set points. The model was also utilized to evaluate the performance under continuous vs staged solvent addition distillation configurations. The full details of the distillation model are not described here; however, similar batch distillation models are fully

dx.doi.org/10.1021/op2003024 | Org. Process Res. Dev. 2012, 16, 567−576

described in the DynoChem software supporting information.[14] Example temperature trends for the distillation of methylene chloride to ethanol under different operating conditions are in Figure 6.

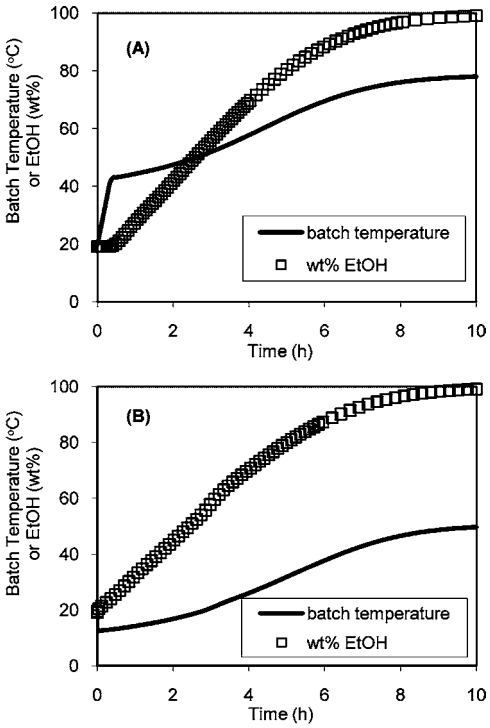

Figure 6. Batch temperature and wt % ethanol trends for distillations at (A) 1013 mbar and (B) 300 mbar.

With the temperature profile defined by the thermodynamic distillation model, several elementary reaction rate equations were postulated to describe the degradation of API enantiomeric purity. The resulting fit of the epimerization kinetics for each rate equation was then compared against 13 epimerization data sets obtained at constant temperature. The rate equation most accurately predicting the system performance is shown below, and the fit to the model building data set is in Figure 7.

$$r_2 = \text{rate of API enantiomeric degradation} = k[\text{API}] \times [2]$$

where $k = k_2 \times \exp(-E_{a,2}/RT)$, $k_2 = 1.90 \times 10^{-3}$ L/mol/s ± 10.8%, $E_{a,2} = 88.2$ kJ/mol ± 12.1%, $T_{ref} = 78$ °C

Combination of the thermodynamic distillation model and the kinetic API enantiopurity degradation model allowed the factors of residual **2**, concentration, distillation temperature, and distillation time to be captured. The model was verified against a set of five additional distillation experiments (Figure 8). Summary error statistics for the model are listed in Table 2. The prediction of the hybrid model is not as accurate as that obtained from the sulfonylation reaction mechanistic model, and the hybrid model is fairly conservative, erring on the side of over-prediction of enantiopurity degradation. Given the stage of development and the intended use for the model predictions in proposing design space conditions to be verified via experiments, this level of model error was deemed acceptable.

Definition of the Design Space and Target Operating Conditions for the 175-kg Pilot-Plant Campaign. *Model Predictions and Data Visualization.* The sulfonylation reaction conversion and the distillative crystallization enantiopurity degradation models were then combined to predict performance across a large process knowledge space (Table 3). Parameter ranges were chosen on the basis of prior process experience to encompass a sufficiently large and practical processing window as well as to contain the expected target-operating conditions. Figure 9 shows two example predictions for reaction conversion and two example predictions for enantiopurity degradation. In total, 1008 predictions for reaction conversion and 432 predictions for enantiopurity degradation were obtained to fully describe the knowledge space shown in Table 3.

While the individual time course reaction trends (Figure 9) were useful for visualizing model predictions from a small number of conditions, we chose to assess the entire knowledge space via two-dimensional contour plots (Figure 10). In order to represent all the data from the four-dimensional knowledge space, groups of contour plots were required. Analysis of the model predictions for sulfonylation reaction conversion across the parameter range considered showed that reaction temperature and equivalents of 4-chlorobenzenesulfonyl chloride had the highest impact on reaction conversion. These parameters were included on the axes of each contour plot. The impact of reaction concentration was lower and was visualized by looking across groups of contour plots where each contour plot was generated for a different reaction concentration. Reaction time was also visualized by looking across groups of contour plots where each plot was generated for a different reaction time. In the case of enantiopurity degradation, the level of residual **2** and the distillation pressure (which is directly correlated to the distillation temperature profile) had the highest impact on % ee loss and were included on the axis of each contour plot. The effects of distillation time and distillation end point can be visualized by looking across groups of contour plots. Representative sulfonylation reaction contour plots are shown in Figure 10 for the lowest reaction conversion, the center point of the knowledge space, and the highest reaction conversion. Representative enantiopurity degradation plots are shown in Figure 10 for the least % ee loss, the center point of the knowledge space, and the highest % ee loss.

Defining a Control Strategy to Simplify Analysis of the Design Space. In order to simplify the representation of the design space for the entire step, we chose to specify a maximum allowable level of **2** at the end of the sulfonylation reaction as the quality gate keeper for the distillative crystallization to be monitored via an in-process-control test (IPC). Remediation under IPC failure would consist of an additional 4-chlorobenzenesulfonyl chloride charge. This allowed the sulfonylation reaction and distillative crystallization to be treated as two independent unit operations and optimized accordingly around a common value of residual **2**. In doing so, we arbitrarily limited the design space to a subset of the acceptable region where residual **2** was less than its maximum level specified, but the advantage in simplification outweighed the additional parameter restrictions. This enabled the focused development of a control strategy targeting residual **2**. Additionally, kinetic understanding of the sulfonylation reaction allowed for conditions to be selected that robustly afforded acceptable reaction conversion.

Determination of the Design Space and Selection of the Desired Operating Conditions. In order to determine the desired operating conditions for the next scale-up campaign, we needed to balance conditions providing robust product quality

dx.doi.org/10.1021/op2003024 | Org. Process Res. Dev. 2012, 16, 567–576

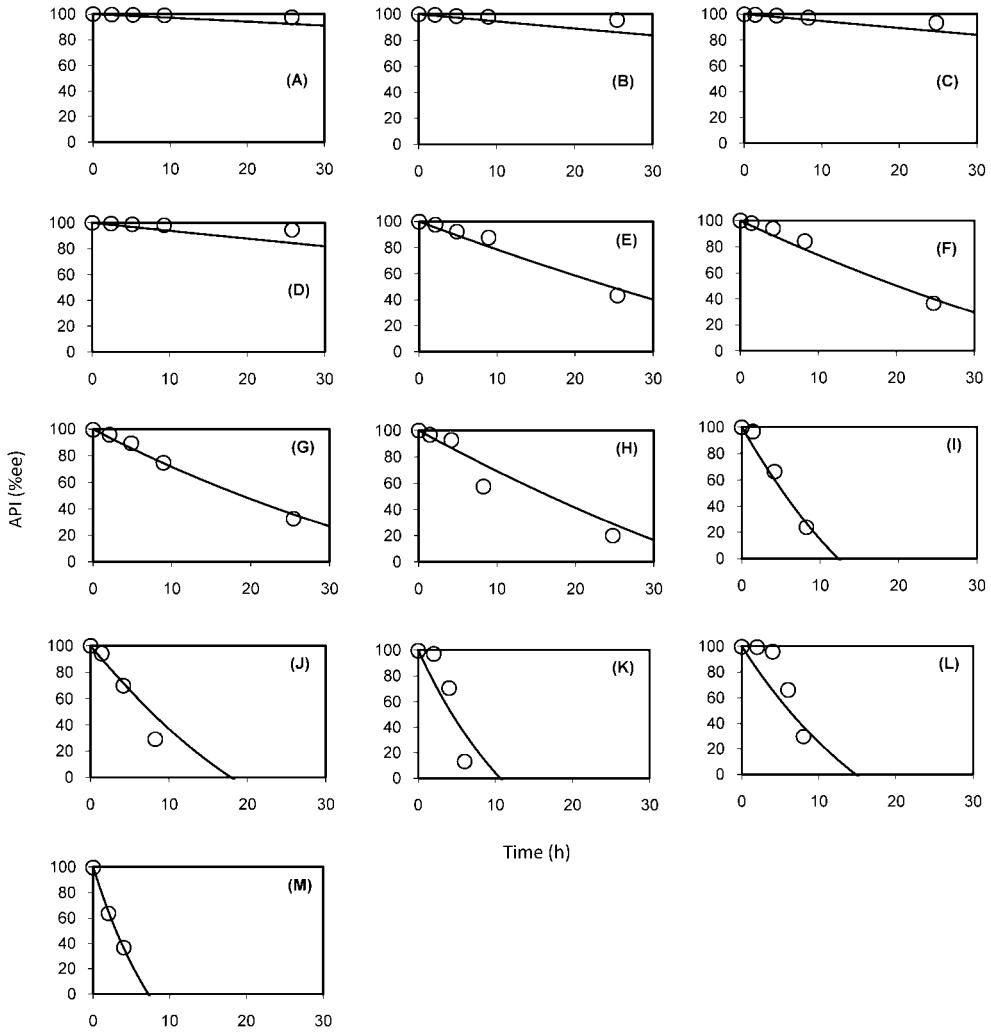

Figure 7. API enantiomeric purity degradation profiles for the 13 model-building experiments. Solid lines represent the model prediction, and open circles represent the experimental values. Experimental temperature and compound **2** conditions are: (A) 45 °C, 1.3 AP; (B) 45 °C, 2.2 AP; (C) 45 °C, 2.5 AP; (D) 45 °C, 2.7 AP; (E) 60 °C, 2.6 AP; (F) 60 °C, 2.6 AP; (G) 60 °C, 3.5 AP; (H) 70 °C, 1.4 AP; (I) 70 °C, 2.3 AP; (J) 70 °C, 2.7 AP; (K) 78 °C, 1.8 AP; (L) 78 °C, 2.5 AP; (M) 78 °C, 3.7 AP.

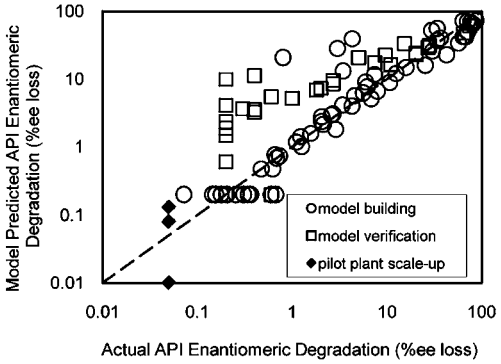

Figure 8. Parity plot for degradation of API enantiomeric purity during the distillative crystallization.

Table 2. Enantiopurity degradation model error for the model building and model verification data sets

	model bldg (entire data set)	model ver. (entire data set)	model bldg (ROI[a])	model ver. (ROI[a])
rms[b] error (% ee)	15.9	8.7	7.9	7.2
mean rel. error (%)	96.0	580.3	133.1	870.5
mean abs. error (% ee)	5.6	5.8	1.9	4.4
max abs. error (% ee)	34.8	17.9	25.1	15.7

[a]For error analysis, the ROI (region of interest) includes points in which the level of API enantiopurity degradation was ≤4.0% ee. [b]rms = root mean square..

with realistic and practical plant operating conditions. From a quality standpoint, purging studies at this point in development suggested that the API crystallization could purge the undesired enantiomer at levels of up to 2% ee. Therefore, the upper boundary on the distillative crystallization design space was set at the red line in Figure 11, A and B, allowing the entire design space to the bottom and left of the red line to be potentially utilized. For example, we could operate the distillation at 300 mbar and produce API meeting its specifications with up to 2.0 AP of residual **2** present during a distillative crystallization lasting 8 h. Alternatively we could drive the sulfonylation

dx.doi.org/10.1021/op2003024 | *Org. Process Res. Dev.* 2012, 16, 567−576

Table 3. Process parameter ranges and number of parameter levels utilized for model-based prediction of sulfonylation reaction conversion and degradation of API enantiopurity during the distillative crystallization

process parameter	min. value	max. value	# of "levels"
sulfonylation reaction model			
temp. (°C)	5	35	7
4-chlorobenzenesulfonyl chloride (equiv)	1.0	1.2	6
conc. (mL/g)	5	10	6
reaction time (h)	2	5	4
distillative crystallization model			
pressure (mbar)	300	1013	6
residual **2** (AP)	0.05	2.0	6
distillation time (h)	8	48	4
distillation end point (wt % EtOH)	90	98	3

reaction to <0.05 AP of **2** and perform the distillation at 300–700 mbar for up to 48 h (Figure 11 B).

Although we had narrowed the distillative crystallization design space on the basis of quality considerations, some regions of the remaining design space were not achievable based on plant capability. From prior knowledge of the equipment train chosen for the next implementation, it was determined that controlling environmental emissions from a methylene chloride distillation operating at <400 mbar was prohibitively expensive. In addition, from the known equipment size and heat transfer coefficients it was established that the total distillation would require approximately 8 h at the proposed batch size. Selecting a conservative distillation end point of 98 wt % EtOH provided a longer distillation time at elevated batch temperatures. Finally, historical performance of the vacuum pressure control system suggested that the distillation could be adequately operated within ±50 mbar of the desired set point without significant concern.

In addition to the constraints on the distillative crystallization, there were also quality, practical, and business constraints on the sulfonylation reaction which were taken into consideration during design space definition. Model results suggested that the reaction conversion limit could be specified as low as <0.05 AP of residual **2** which would provide the largest design space for the distillative crystallization; however, doing so would result in a much smaller design space for the sulfonylation reaction (high temperature, long reaction times, high equivalents of reagent). From a quality standpoint, unreacted 4-chlorobenzenesulfonyl chloride could form a genotoxic sulfonate ester during the distillative crystallization; therefore, using greater than 1.2 equiv of 4-chlorobenzenesulfonyl chloride was undesired. From a business standpoint, reaction times of greater than 24 h would be needed at the 5 °C temperature conditions to achieve <0.05 AP of residual **2**, thus limiting plant throughput.

After considering all the factors listed above and balancing the sizes of the sulfonylation reaction and distillative crystallization design spaces, we chose to operate the distillation for the pilot-plant campaign at 500 mbar. Given a pressure control range of ±50 mbar, this allowed up to 1 AP of residual **2** to be present at the end of the sulfonylation reaction (Figure 12A). To achieve this level of reaction conversion, we needed to operate the sulfonylation reaction within the design space shown in Figure 12B. The manufacture of clinical supplies at the pilot scale provides an opportunity to test the scale independence of the process and the ability of the process

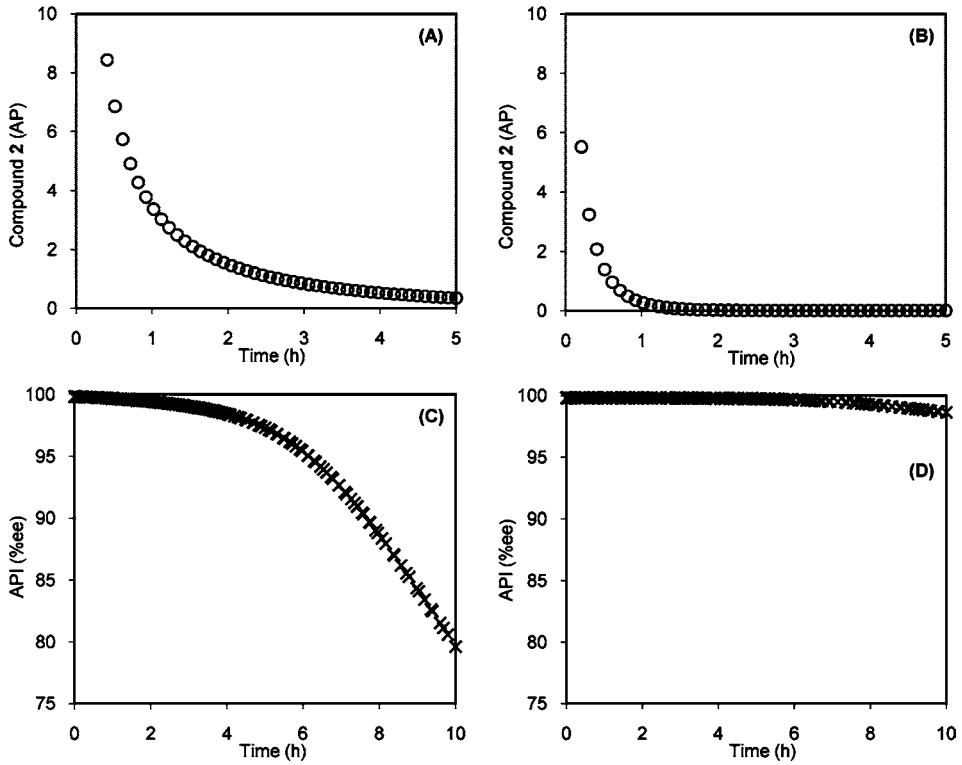

Figure 9. Sulfonylation reaction conversion predictions for (A) 10 °C, 1.03 equiv of 4-chlorobenzenesulfonyl chloride, 4.5 mL/g and (B) 35 °C, 1.10 equiv of 4-chlorobenzenesulfonyl chloride, 10 mL/g. API enantiomeric purity predictions for (C) 1 AP of residual **2**, 1013 mbar and (D) 1 AP of residual **2**, 300 mbar.

dx.doi.org/10.1021/op2003024 | *Org. Process Res. Dev.* 2012, 16, 567–576

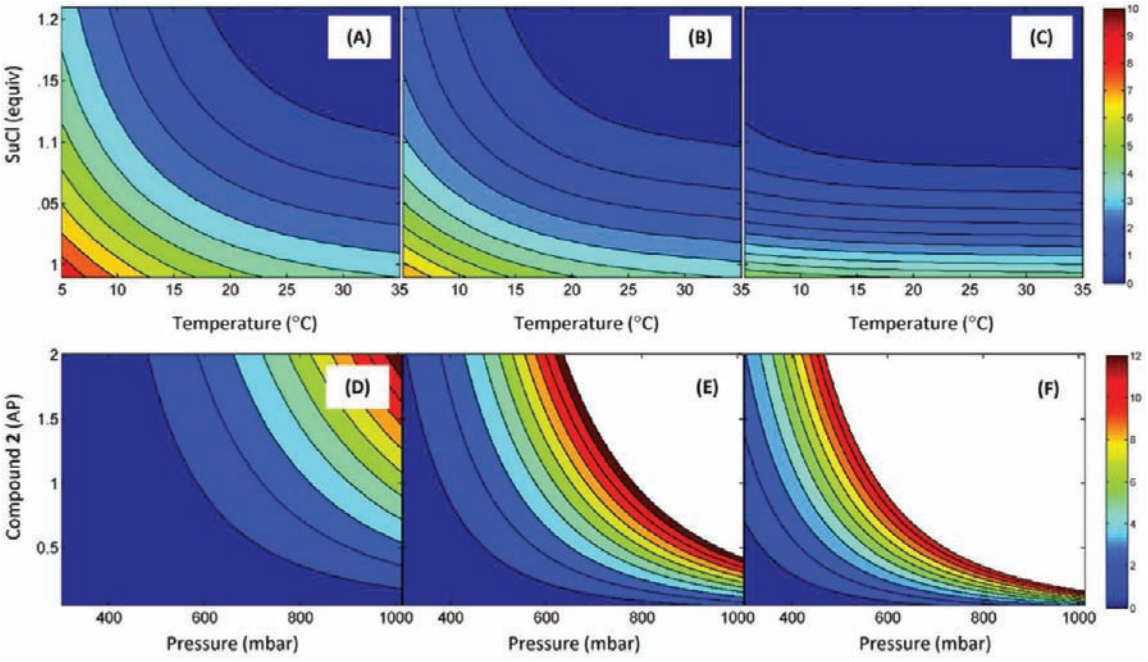

Figure 10. Representative two-dimensional contour plots. Sulfonylation reaction model predictions for residual level of **2** shown in the color contrast at (A) the lowest reaction conversion, 10 mL/g dilution, 2 h reaction, (B) the center of the parameter range, 7 mL/g, 2 h reaction, and (C) the highest reaction conversion, 5 mL/g, 5 h reaction. Model predictions for API enantiopurity degradation shown in the color contrast at (D) the least amount of degradation, 90 wt % EtOH end point, 8 h distillation, (E) the center of the parameter range, 95 wt % EtOH end point, 24 h distillation, and (F) the highest amount of degradation, 98 wt % EtOH end point, 48 h distillation. For clarity, values of greater than 12% ee loss have been removed from the graphical representation.

models to predict performance during scale-up. In order to confirm our model predictions, we chose to operate the three scale-up batches at distinct points within the sulfonylation reaction and distillative crystallization design spaces as shown by the target operating conditions in Table 4. This table also contains the outcome from the pilot-plant campaign and comparison of the scale-up results to the model predictions. In summary, by using this model-based approach we were able to define a process design space capable of producing API at the expected purity and yield, without any detectable enantiomeric degradation. Additionally, the agreement between the actual results obtained and the results predicted by the model provided confidence that the model could be accurately used to determine the edges of failure and to guide further definition of the design space going forward.

Generation of Additional Process Knowledge and Revision of the Design Spaces and Target Operating Ranges for Future Campaigns. While the 175-kg pilot-plant campaign successfully produced API meeting all of the quality specifications, additional development work was focused on preparation for future campaigns and the ultimate transfer of the process to manufacturing. Systematic evaluation of the crystallization revealed the existence of a stable racemic compound with an eutectic point of 86% ee. Therefore, the thermodynamic purification of the crystallization at the current yield was only 0.9% ee, rather than ≥2% ee as was previously demonstrated. As a result, the design spaces for the sulfonylation reaction and distillative crystallization required adjustment. Additionally, new data were being collected to improve the predictive capability of the model for the degradation of enantiomeric purity, with specific focus on accuracy within the small levels of ee degradation required (0–1% ee loss). This work revealed that in the three experiments where ee degradation was the most overpredicted by the model, a higher than expected level of 4-chlorobenzenesulfonic acid was present (degradation product of 4-chlorobenzenesulfonyl chloride) during the distillative crystallization. This finding suggested that robustness during the distillative crystallization could be improved by implementing a pH specification on the workup. It was also anticipated that a modification of the ee degradation model would be required to capture the reduced rate of racemization.

In parallel with the collection of additional process data and improvements in the models' predictive capabilities, the existing models enabled design space decisions and provided parameter settings for additional data collection to ensure process (and therefore model) insensitivity to scale-up. Following the methodology summarized in Figure 13, model-based predictions of the critical quality attributes provided the desired operating conditions and ranges for the 175-kg campaign and enabled the process risk assessment. When combined with differences in operating preferences (for example an atmospheric distillation vs a vacuum distillation) and control capabilities at a new scale-up facility, the process models were used to predict CQA performance for the next campaign. Future work would have focused on verifying these predictions via lab-scale experiments and scale-up batches and utilizing the results in the next round of process risk assessments. Throughout these experiments, we had planned to track CQA performance, process reproducibility, process robustness, and process scalability to support the ultimate regulatory filing(s). In an approach similar to that previously described by Seibert et al.,[4] critical process parameters (CPP) would have been identified via analysis of the plant control capabilities for each individual parameter against the parameter's acceptable range as described by the process design space. Parameters for

dx.doi.org/10.1021/op2003024 | *Org. Process Res. Dev.* 2012, 16, 567–576

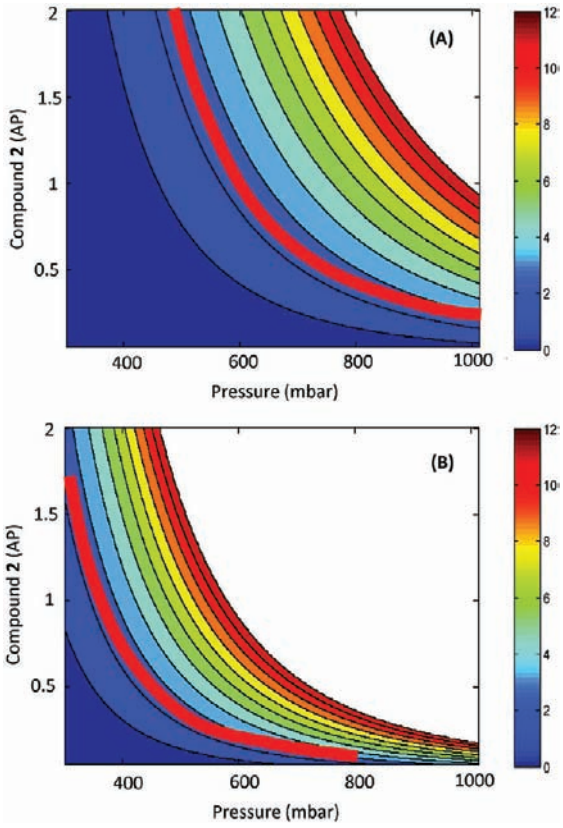

Figure 11. Definition of the design space for the distillative crystallization based only on quality considerations. The level of enantiopurity degradation is shown in the color contrast at (A) 8 h distillation, 98 wt % EtOH end point, and (B) 48 h distillation, 98 wt % EtOH end point. On the basis of crystallization purge data, conditions to the left and below the red line are expected to provide acceptable quality API. For clarity, values of greater than 12% ee loss have been removed from the graphical representation.

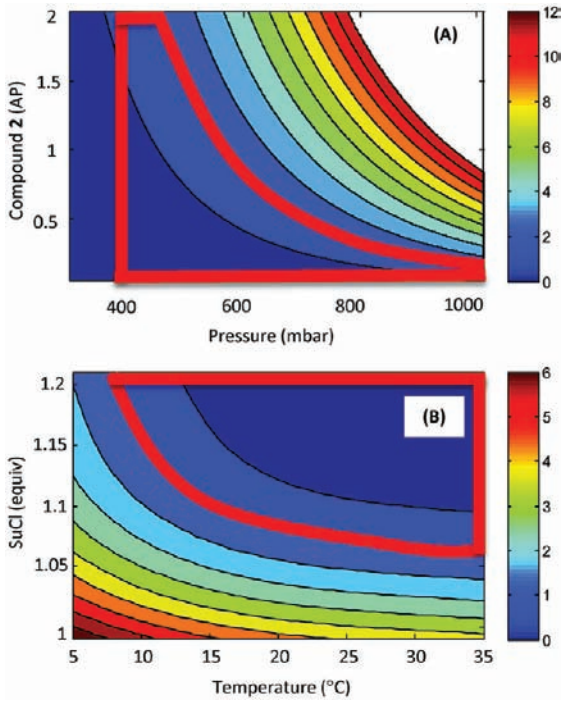

Figure 12. Finalized design space for the distillative crystallization (A) and sulfonylation reaction (B) after consideration of product quality, realistic plant operating conditions, plant control capabilities, and business drivers. (A) Level of enantiopurity degradation is shown in the color contrast at the end of an 8 h distillation to a 98 wt % EtOH end point. For clarity values of greater than 12% ee loss have been removed from the graphical representation. (B) Level of residual **2** is shown in the color contrast for the sulfonylation reaction at 2 h and a volume of 7 mL/g.

which a risk existed that could not be controlled within the design space would have been identified as CPPs. Although the end goal with respect to the definition and verification of the design space for the commercial process had not yet been fully defined, we had envisioned two possible approaches. In one approach, similar to that described by Hallow et al.,[15] the process models would have served as a guide for selection of the design space which would have been verified via experiments. In a second approach, similar to that described by Chen et al.,[16] the verified process models themselves would have defined the design space.

CONCLUSION

This case study details one example of a process modeling-based work flow for QbD. Starting from data mining and risk evaluation of the existing experimental data set, aspects of the process which were potentially critical to quality were identified. Although the general approach to QbD is typically to engage in a design of experiments endeavor, in this case the quality, quantity, and scope of the historical data were deemed sufficient to attempt the development of mechanistic models in the absence of a target experimental design. The models were developed and were able to simulate and predict the failure modes observed within the historical data set. On the basis of a risk assessment and the stage of development, model predictions were verified via lab-scale experiments and the process models were then used to predict performance across the entire parameter range. Model predictions were combined with the anticipated acceptable quality attributes, practical plant

Table 4. Processing conditions chosen for the 175-kg pilot-plant campaign and the resulting reaction conversion and enantiopurity degradation results

	batch #1	batch #2	batch #3
Sulfonylation Reaction			
batch size (kg)	50	60	90
temp. (°C)	20 (19.9–25.3)	10 (9.5–16.4)	30 (30.1–34.6)
4-chlorobenzenesulfonyl chloride (equiv)	1.15	1.18	1.12
conc. (mL/g)	6	5.5	8
reaction time (h)	2.5	2.5	2.5
model-predicted residual cmpd **2** (AP)	0.12	0.17	0.15
actual cmpd **2** (AP)	0.04	0.18	0.07
Distillative Crystallization			
pressure (mbar)	500 (353–560)	500 (490–526)	500 (485–544)
distillation time (h)	5.5	2.8	6.3
distillation end point (wt % EtOH)	94.9	90.6	97.9
predicted ee degradation (% ee loss)	0.00	0.08	0.13
actual ee degradation (% ee loss)	<0.1	<0.1	<0.1

dx.doi.org/10.1021/op2003024 | *Org. Process Res. Dev.* 2012, 16, 567–576

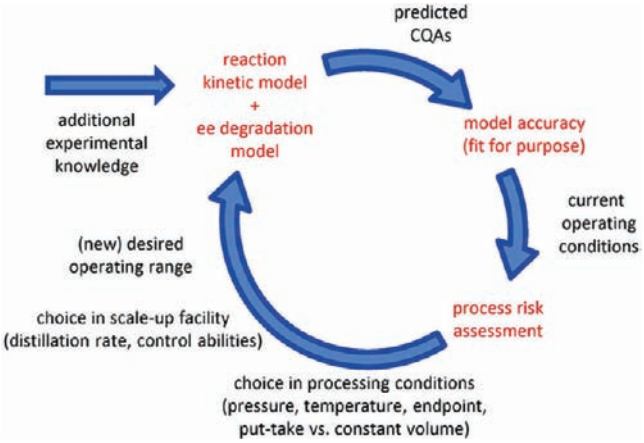

Figure 13. Modeling-based QbD methodology employed in this case study.

operating conditions, and plant control capabilities to propose a process design space. Further analysis of business goals (process throughput and yield) defined the target operating conditions and normal operating ranges for a specific scale-up campaign. Model results were then compared to at-scale data, and the model assumptions were reevaluated in preparation for the subsequent scale-up campaign.

In this case study, targeted experimental designs were not performed; rather, the data for model development were gathered primarily from existing lab experiments originally performed for other purposes. In doing so, unknown parameter interactions or interactions assumed insignificant were not captured; however, consistency between the model predictions and the experimental data suggests the models adequately represent the underlying physical mechanisms. Additionally, parameters within the experimental data set were not varied in a systematic manner as they would have been within a DOE. As a result, model performance must be verified according to risk, and we chose to do so via experimental verification at the design space extremes as well as at the target operating conditions. In the end, the development of verified process models drove the aggregation of data collected under dramatically different process conditions, allowed the rapid generation of response surfaces, justified QbD-related decisions, and enabled in-depth evaluation of the scale-up data obtained.

AUTHOR INFORMATION

Corresponding Author

*E-mail: shawn.brueggemeier@bms.com.

Notes

The authors declare no competing financial interest.

ACKNOWLEDGMENTS

We acknowledge Jean Tom, Scott Jones, Rajendra Deshpande, and San Kiang for their support, guidance, and helpful discussions. We also acknowledge Alexander Marchut, Brenda Remy, Susanne Kiau, Li Li, Peter Tattersall, Landon Greene, Alan Braem, Justin Burt, Randy Ferrari, Jeffrey Zelenkow, and George Toropiw for their contributions. Finally, we acknowledge Joe Hannon of Scale-up Systems Ltd. for the support with development of the DynoChem models.

REFERENCES

(1) Garcia, T.; Cook, G.; Nosal, R. *J. Pharm. Innov.* **2008**, *3*, 60−68.
(2) Lepore, J.; Spavins, J. *J. Pharm. Innov.* **2008**, *3*, 79−87.
(3) Ganzer, W. P.; Materna, J. A.; Mitchell, M. B.; Wall, L. K. *Pharm. Technol.* **2005**, *July*, 2.
(4) Seibert, K. D.; Sethuraman, S.; Mitchell, J. D.; Griffiths, K. L.; McGarvey, B. *J. Pharm. Innov.* **2008**, *3*, 105−112.
(5) *ICH Q8 Pharmaceutical Development*; U.S. Department of Health and Human Services, Food and Drug Administration, Center for Drug Evaluation and Research (CDER): Rockville, MD, August 2009.
(6) *ICH Q9 Quality Risk Management*; U.S. Department of Health and Human Services, Food and Drug Administration, Center for Drug Evaluation and Research (CDER): Rockville, MD, June 2006.
(7) *ICH Q10 Pharmaceutical Quality System*; U.S. Department of Health and Human Services, Food and Drug Administration, Center for Drug Evaluation and Research (CDER): Rockville, MD, April 2009.
(8) Castagnoli, C.; Yahyah, M.; Cimarosti, Z.; Peterson, J. J. *Org. Process. Res. Dev.* **2010**, *14*, 1407−1419.
(9) am Ende, D.; Bronk, K. S.; Mustakis, J.; O'Connor, G.; Santa Maria, C. L.; Nosal, R.; Watson, T. J. N. *J. Pharm. Innov.* **2007**, *2*, 71−86.
(10) Lange, J. H. M.; van Stuivenberg, H. H.; Veerman, W.; Wals, H. C.; Stork, B.; Coolen, H. K. A. C.; McCreary, A. C.; Tiny, J. P.; Kruse, C. G. *Bioorg. Med. Chem. Lett.* **2005**, *15*, 4794−4798.
(11) Lange, J. H. M.; Coolen, H. K. A. C.; van Stuivenberg, H. H.; Dijksman, J. A. R.; Herremans, A. H. J.; Ronken, E.; Keiver, H. G.; Tipker, K.; McCreary, A. C.; Veerman, W.; Wals, H. C.; Stork, B.; Vereer, P. C.; den Hartog, A. P.; de Jong, N. M. J.; Adolfs, T. J. P.; Hoogendoorn, J.; Kruse, C. G. *J. Med. Chem.* **2004**, *47*, 627−643.
(12) The 4-chlorobenzenesulfonyl chloride was added all at once during the reaction, and therefore addition time is not included as a factor in the Ishikawa diagram.
(13) Enantiopurity degradation could also occur during drying as described in the Ishikawa diagram; however, this factor is not included in the analysis as the drying operating range was well within the temperature range for API enantiopurity stability.
(14) Model Library - Batch Distillation - Solvent Switch Model. *DynoChem 2008 Software*, version 3.3; Scale-up Systems Ltd.: Dublin, Ireland, 2008.
(15) Hallow, D. M.; Mudryk, B. M.; Braem, A. D.; Tabora, J. E.; Lyngberg, O. K.; Bergum, J. S.; Rossano, L. T.; Tummala, S. *J. Pharm. Innov* **2010**, *5*, 193−203.
(16) Chen, W.; Chang, S. Y.; Kiang, S.; Marchut, A.; Lyngberg, O.; Wang, J.; Rao, V.; Desai, L.; Stamato, H.; Early, W. *J. Pharm. Sci.* **2010**, *99*, 3213−3225.